01

The concept of unit cells in the theory of quasicrystals

© A.E. Madison,[1] P.A. Madison,[1,2] V.A. Moshnikov[2]

[1] National Research University Higher School of Economics,
190121 St. Petersburg, Russia
[2] St. Petersburg State Electrotechnical University „LETI",
197022 St. Petersburg, Russia

e-mail: alex_madison@mail.ru

Received November 15, 2023
Revised December 22, 2023
Accepted December 28, 2023

To describe the structure of icosahedral quasicrystals, the concept of (quasi-)unit cells is proposed as an alternative to the higher-dimensional approach. The problem of describing the structure of icosahedral quasicrystals splits into two stages: filling the cells with atoms and filling the space with cells. The only difference from ordinary periodic crystals is that four unit cells should be used instead of one, and an iterative inflation/deflation algorithm should be used instead of translations to fill the entire space with cells. Icosahedral packings are described as lists of cells, each of which is given its type, position, and orientation. Based on the developed algorithm, representative fragments of all three types of the Socolar–Steinhardt zonohedral packing were generated, which clearly illustrate the main structural features and hierarchical motifs of icosahedral quasicrystals. The theoretical possibility of calculating the intensities of X-ray reflections in the structural analysis of quasicrystals without using the higher-dimensional crystallography approaches is discussed. To do this, one should first calculate the partial structure factors for each type of unit cell, and then average them over the volume of the quasicrystal by using the derived substitution rules.

Keywords: icosahedral quasicrystals, substitution rules, zonohedra, packing.

DOI: 10.61011/JTF.2024.04.57526.284-23

Introduction

The discovery of icosahedral quasicrystals [1] is one of the milestones in modern crystallography. The notion of a crystal now encompasses the possibility of both periodic and aperiodic ordering. The first theoretical interpretation of long-range ordering in structures with an icosahedral symmetry has been provided in [2,3], where a tiling of three-dimensional space with four types of „golden" zonohedra (zonohedral Socolar–Steinhardt tiling) was considered.

At present, the atomic structure of quasicrystals is normally characterized within higher-dimensional crystallography by projection of 3D-cuts of higher-dimensional lattices into physical space [4,5]. This approach relies on expanding the quasicrystalline density function into a Fourier series with the number of reciprocal space basis vectors exceeding the physical space dimensionality. The actual results of a diffraction experiment are normally used as Fourier coefficients. If a material has not been synthesized yet and its probable structure is to be predicted, the cut-and-project method encounters significant difficulties.

The higher-dimensional approach has been proven efficient in refinement of the structures of multicomponent quasicrystalline alloys with icosahedral symmetry. The structure is refined by fitting the calculated intensities of diffraction reflections to experimental ones within a certain pre-selected model structure. A model with mutually overlapping rhombic triacontahedra [6–8] is used widely. Note that, in all likelihood, this model ensures neither an exact icosahedral symmetry nor self-similarity in the context of long-range ordering. Intriguingly, the Socolar–Steinhardt tiling itself was also obtained by projection from 6D-space (and, consequently, agrees completely with the higher-dimensional approach), provides a unique reproduction of icosahedral long-range order, and satisfies completely the self-similarity criterion, but has almost never been used for the refinement of structures of actual quasicrystalline alloys. This may be attributed to long-standing difficulties in implementing the algorithm of its construction.

The interest in photonic quasicrystals and quasicrystalline materials from non-atom building blocks has been on the rise lately [9–14]. An alternative approach based on the inflations and deflations of quasi-unit cells may be a better fit in this case [15]. Specifically, a set of four „golden" zonohedra may be used as such cells.

Recently, we have derived substitution rules for the zonohedral Socolar–Steinhardt tiling and developed an efficient iterative algorithm for generation of icosahedral packings based on them [16–20]. This algorithm was optimized fairly well, providing an opportunity for relatively fast generation of large patterns of icosahedral packings containing tens of millions of unit cells. The aim of the present study is to illustrate the structural features of icosahedral packings and demonstrate that icosahedral quasicrystals may be regarded as self-similar packings of unit cells.

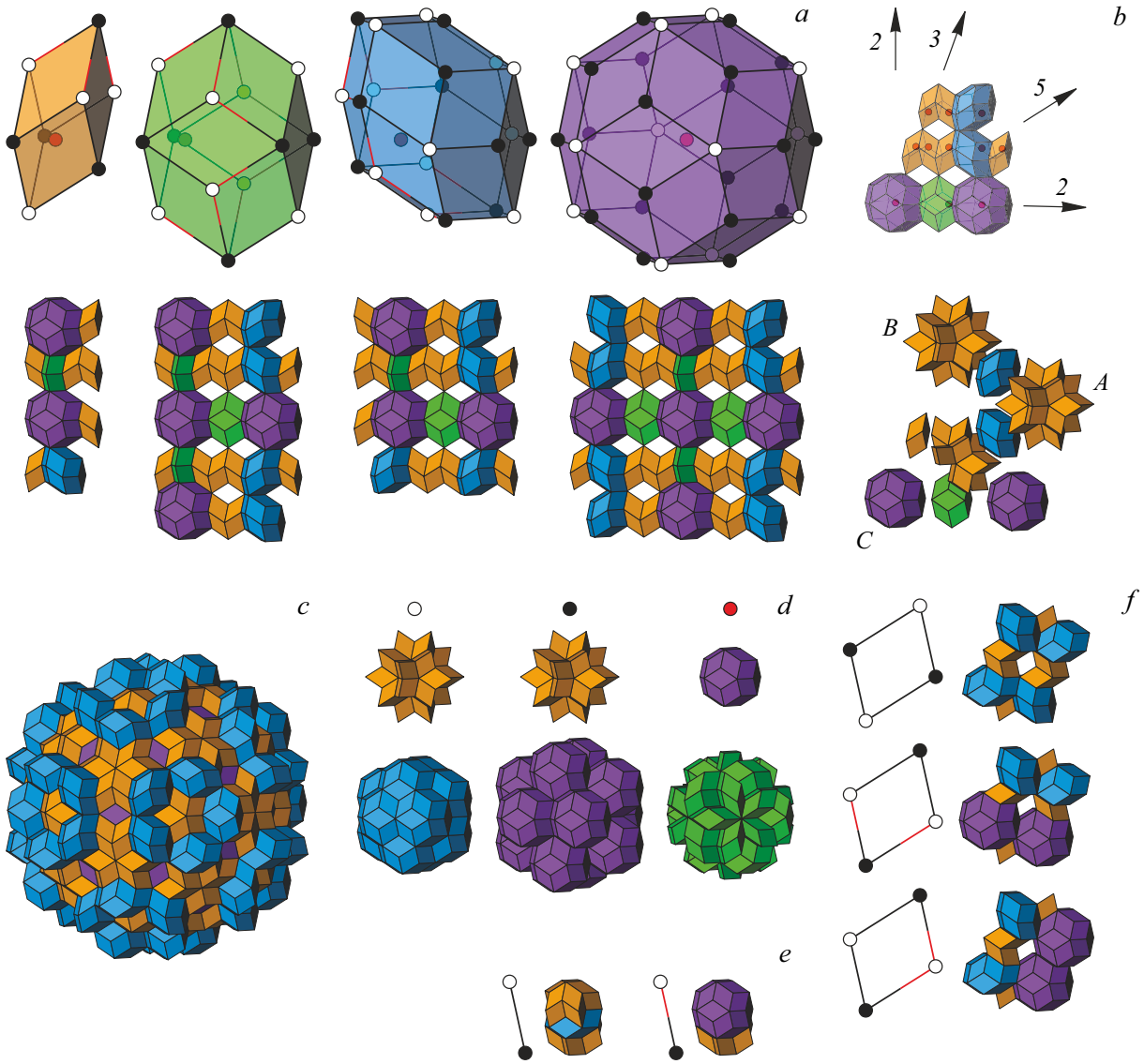

Figure 1. Principles of construction of icosahedral packings: *a* — four types of unit cells (prolate rhombohedron, rhombic dodecahedron, rhombic icosahedron, and triacontahedron) and illustration of substitution rules for them (layers are cut perpendicular to the global 2-fold axis); *b* — minimal set of 12 zonohedra underlying the substitution rules and illustration of mutual arrangement of three types of inequivalent sites; *c* — triacontahedron deflation rule, which includes a total of 533 polyhedra; *d* — three types of inequivalent sites and three corresponding ways to initialize the algorithm for construction of all three types of locally isomorphic icosahedral packings. Natural local matching rules: *e* — two types of edges; *f* — three types of faces.

1. Algorithm for construction of icosahedral packings

The concept of (quasi-) unit cells has an obvious counterpart in classical crystallography. The structure of a common periodic crystal may be characterized by its unit cell with atoms in certain locations, which is then replicated with the use of a three-dimensional translation subgroup to cover the entire space. The structure of icosahedral quasicrystals may be characterized in much the same way. The difference is that four unit cells need to be used instead of a single one and an iterative inflation and deflation algorithm should be used instead of translations to fill the entire space with cells.

Thus, the problem of characterizing the structure of icosahedral quasicrystals splits into two steps: filling of cells with atoms and filling of space with cells.

Our approach is based on the zonohedral Socolar–Steinhardt tiling. The algorithm of its construction is illustrated in Fig. 1. There are four types of unit cells: prolate rhombohedron, rhombic Bilinski dodecahedron, rhombic Fedorov icosahedron, and rhombic Kepler triacontahedron (Fig. 1, *a*). They fill the entire space face-to-face without gaps and overlaps. Any cell in a global packing is defined by its type, position, and orientation.

A packing is generated by applying the inflation–deflation algorithm to a certain valid initial configuration of unit cells.

At the first step, four types of zonohedra are enlarged by a given scale factor (i.e., inflation operation is performed). It is worth reminding that the self-similarity factor for icosahedral quasicrystals depends on the type of the generating 6*D*-lattice and is equal to τ^3 (for the P-type lattice) or τ (for I- and F-type lattices), where τ is the golden ratio [21]. The scale factor for the Socolar–Steinhardt tiling is τ^3. At the second step, the obtained supercells are filled with copies of cells of the initial size in accordance with substitution (deflation) rules. This process is then repeated.

A minimal base configuration of 12 zonohedra (Fig. 1, *b*) underlies the substitution rules derived in our study [16]. Another rhombohedron is added to this configuration if one forms characteristic stars of rhombohedra around the corresponding vertices of enlarged cells. The minimal set of polyhedra is then replicated under the group action of the icosahedral symmetry group. The resulting triacontahedron deflation rule includes a total of 533 polyhedra of different types and orientations (Fig. 1, *c*); notably, some of them are shared by several adjacent supercells in the global packing.

Substitution rules for smaller zonohedra are derived from the corresponding rule for the triacontahedron. Socolar and Steinhardt have demonstrated that zonohedra may be subdivided into smaller parts by Ammann planes [3]. It then turns out that zonohedra consist of matching fragments. It is natural to assume that the substitution rules for matching fragments should also match. In other words, to obtain substitution rules for all the other zonohedra, one needs just to superimpose them over a deflated triacontahedron and copy the polyhedra located within it; the only thing left is then to add several missing polyhedra in such a way as to form the corresponding stars of rhombohedra at the vertices of supercells. Figure 1, *a* illustrates the resulting substitution rules: four types of zonohedra after inflation are shown in the upper row, and the result of their deflation is present below (layers cut perpendicular to the global 2-fold axis are shown). It is important to take local matching rules into account and maintain the correct orientation of polyhedra when zonohedra are deflated, since the geometric centers of all zonohedra (except for a triacontahedron) are not their centers of the inversion symmetry.

The derived substitution rules [16] guarantee that the generated packing is self-similar with the scale factor of τ^3. The icosahedral symmetry of global packing is preserved after each iteration, as well as after the decoration of cells with atoms. Deflation rules for different zonohedra are consistent with each other so as to exclude conflicts at all stages of deflation of adjacent cells. Applying the inflation and deflation operations in turns to any zonohedron or to any valid configuration of zonohedra, one may fill a region of arbitrarily chosen size with cells. The tiling is similar to the Penrose tiling in being locally isomorphic.

Deflation rules provide an opportunity to formulate the so-called natural local matching rules, which postulate the existence of three types of inequivalent cites (Fig. 1, *d*), two types of edges (Fig. 1, *e*), and three types of faces (Fig. 1, *f*) in the packing. In the course of packing, the shared vertices, edges and faces of adjoining cells should always be of the same type. These requirements are in agreement with the decoration of faces by Ammann planes in the higher-dimensional approach [3].

Zonohedra have two types of vertices, which are designated as *A*- and *B*-type ones. Edges always connect vertices of alternate types. After several iterations, any vertex of the type *A* turns into a star of rhombohedra surrounded by rhombic icosahedra, and any vertex of the type *B* turns into a similar star of rhombohedra, which are differently oriented (assembled around the opposite vertex) and surrounded by triacontahedra. Type *C* sites correspond to local origins of zonohedra (coincide with the local origin of the local coordinate system of the corresponding zonohedron). After several iterations, a *C*-type cite turns into a triacontahedron surrounded by rhombic dodecahedra.

Let us clarify the packing generation algorithm. As was already noted, the type, position, and orientation should be specified for any cell. All substitution rules, initial cell configurations, packings obtained both at intermediate stages after each successive iteration and at the final stage, and layers cut from them in different ways may then be considered as lists of cells.

The cell type is an integer number that corresponds to one of the four types of zonohedra. The position of a specific zonohedron is set by the coordinates of its local origin in the global reference frame and is specified by six integers. This is related to the fact that the coordinates of all vertices and local origins of all cells are algebraic integers if the reference frame and measurement units are chosen correctly. They belong to ring of integers $\mathbb{Z}[(1+\sqrt{5})/2]$ of quadratic field $\mathbb{Q}(\sqrt{5})$. In other words, the coordinates of any *A*-, *B*-, or *C*-type node in any correctly generated icosahedral packing are specified by binomial expressions of the $m+n\tau$ form with integer coefficients [20].

The spatial orientation of a cell is specified by its rotation relative to a certain preselected reference orientation (i.e., by the number of a certain element of icosahedral symmetry group I). The determination of possible spatial orientations of zonohedra corresponds to the problem of decomposition of the icosahedral symmetry group onto left cosets with respect to a given stabilizer subgroup [20].

For example, the stabilizer subgroup of a rhombic icosahedron is generated by a 5-fold axis and its powers. It defines the inner cell symmetry (i.e., the rules of filling it with atoms). Corresponding left cosets define 12 possible spatial orientations of a rhombic icosahedron (i.e., the orbit of a cell with respect to its stabilizer). Likewise, the stabilizer subgroup of a prolate rhombohedron is generated by a 3-fold axis, and the corresponding orbit defines its 20 possible orientations. The stabilizer subgroup of a rhombic dodecahedron is generated by a 2-fold axis, and the corresponding orbit defines its 30 possible orientations.

The packing generation algorithm thus assumes a very simple form:

$$\mathbf{R}_k = \tau^3 \mathbf{R}_i + g_i \mathbf{R}_j,$$

$$g_k = g_i g_j.$$

Here, $\mathbf{R}_i$ and g_i denote the position and orientation of a generating (parent) cell, $\mathbf{R}_j$ and g_j denote the position and orientation of a generated (daughter) cell in the deflation scheme for the standard parent cell orientation, and $\mathbf{R}_k$ and g_k denote the position and orientation of a generated cell in the global packing. The efficiency of this algorithm increases significantly if one uses the multiplication table of the icosahedral group instead of multiplying rotation matrices and uses multiplication in the ring of algebraic integers instead of floating-point operations when calculating the coordinates.

A search through the elements of the input list is performed at each iteration. The needed substitution rule is actuated depending on the cell type, and daughter cells are generated accordingly using the above formulae and added to the output list. At the end of iteration, the list is ordered and duplicate records are removed. The resulting lists of cells are used for the graphical visualization of the packings.

2. Characteristic features of icosahedral packing of zonohedra

Just three different zonohedral packings with an exact icosahedral point symmetry filling the entire three-dimensional space are known to exist. Notably, they are all locally isomorphic to each other. The available data on them have long been limited to the first two coordination spheres: a star of rhombohedra surrounded by rhombic icosahedra, a star of rhombohedra surrounded by triacontahedra, and a triacontahedron surrounded by rhombic dodecahedra [3]. We have demonstrated that all of them are generated by a common algorithm [16–18]. The sole difference is in the choice of an initial configuration.

Let us consider a single rhombohedron and replicate it by the group action to form a star of rhombohedra. A star of 20 rhombohedra (rhombic hexecontahedron) is the complete orbit of a single rhombohedron in the icosahedral symmetry group. Note that the rhombohedron itself is asymmetric and its local origin (cite of the type C) does not coincide with the geometric center of a cell (Fig. 1, a). Node C divides the principal diagonal [AB] in the ratio $1:\tau$ and is located closer to vertex A. Therefore, there are two non-equivalent ways to form a star of rhombohedra. If one groups 20 rhombohedra around vertex A and uses the obtained configuration as the initial one for the inflation–deflation algorithm, the first desired packing (with its origin at node A) is derived. If 20 rhombohedra are grouped around the opposite vertex, the second desired packing (with its origin at node B) is obtained. If a single triacontahedron is used as the initial configuration, the third and final desired packing (with its origin at node C) is found.

Having analyzed the obtained packings, we identified their characteristic structural motifs and certain intriguing features of icosahedral packings in general. The results are presented below in Figs. 2–9.

Figures 2, 3 illustrate the packing centered at node A. Two consecutive layers cut perpendicular to the 5-fold axis are shown. Only rhombohedra are present in the first layer (Fig. 2). The second layer (Fig. 3) is located above the first one.

Figures 4–6 illustrate the packing centered at node B. As above, two consecutive layers are shown. Figure 4 presents the first layer with only the rhombohedra left in it. Differences in the local environment of nodes A and B generated from the same rhombohedron become evident. This is yet another indication that the inclusion of asymmetry of unit cells is crucial. If one takes all types of polyhedra into consideration, the first layer assumes the form presented in Fig. 5. The second layer (Fig. 6) is located above the first one.

Figures 7–9 illustrate the packing centered at node C. As above, two consecutive layers are shown. Figure 7 presents the first layer with only the triacontahedra left in it. The first layer with all types of polyhedra included is shown in Fig. 8. The second layer (Fig. 9) is located above the first one.

Such representation of results with only one type of cells left in a layer (specifically, those ones that generate the whole layer) allows one to reveal the features of hierarchical structure of quasicrystal packings. If one fills unit cells with specific atoms in accordance with certain rules [20], icosahedral clusters of three different types should actually emerge at nodes A, B and C. Figures 2, 4, and 7 demonstrate the mutual spatial arrangement of these clusters. Note that the arrangement of triacontahedra around the central triacontahedron exactly reproduces the mutual arrangement of Tsai clusters [7]. It should be highlighted that the structural motifs of hierarchical clusters (superclusters, clusters of clusters) are characteristic of the packing in general and should not depend on the specific method of decoration of cells with atoms. In addition, the knowledge of hierarchical structural features of superclusters provides an opportunity to compare icosahedral packings constructed from different basis sets of polyhedra.

Thus, icosahedral packings of zonohedra feature strict long-range ordering and are examples of deterministic aperiodic structures. It is our belief that the structure of any ideal icosahedral quasicrystal may be characterized within the concept of unit cells. To do this, one needs just to fill unit cells with specific atoms.

3. Averaging over the packing volume with the use of substitution rules

Let us assume that four types of cells are filled with atoms in a certain specific way and the 3D-structure of an

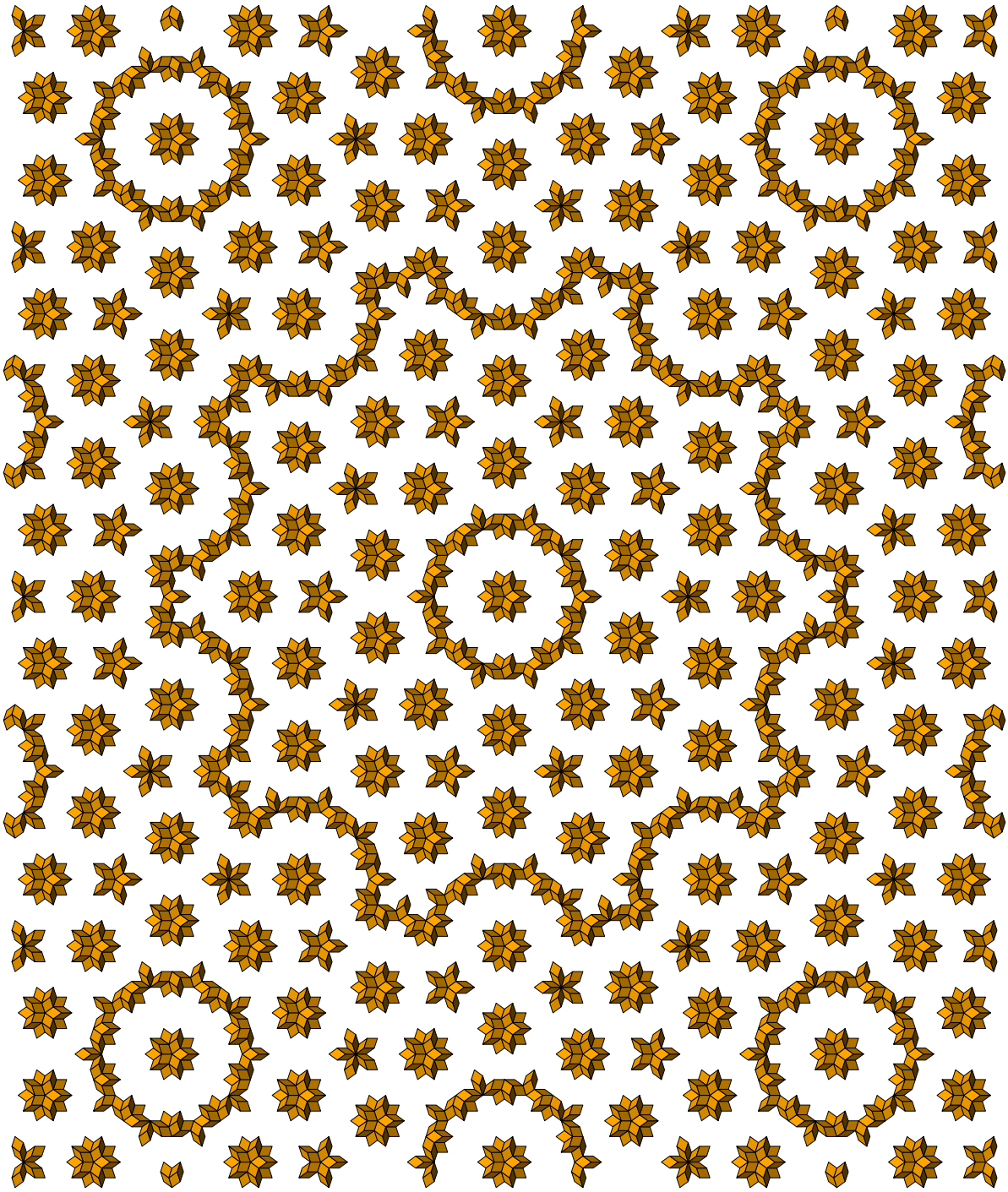

Figure 2. Icosahedral packing of zonohedra. The packing is centered at the type A node, and the layer is cut perpendicular to the 5-fold axis. The first layer of polyhedra is shown.

ideal quasicrystal is constructed. What is the density of the obtained packing? What is its stoichiometric composition? For a common periodic crystal, the answer is trivial: in order to calculate the crystal density, one needs to find the sum of masses of all atoms in a unit cell and divide it by the cell volume. Is there a similar method for quasicrystals? According to our research [19,20], the answer is positive. This sought-for method relies on the application of Perron projection to the (transposed) substitution matrix of the Socolar–Steinhardt tiling.

Let us elaborate on the above points. Substitution matrix $\mathbf{M}$ for the Socolar–Steinhardt tiling has been obtained in our earlier study [16]. Substitution matrix elements M_{ij} indicate the number of subcells of the type i in a supercell of the type j. Let us multiply transposed matrix $\mathbf{M}^{\mathrm{T}}$ by column vector $\mathbf{v}$ of cell volumes. It is assumed that the

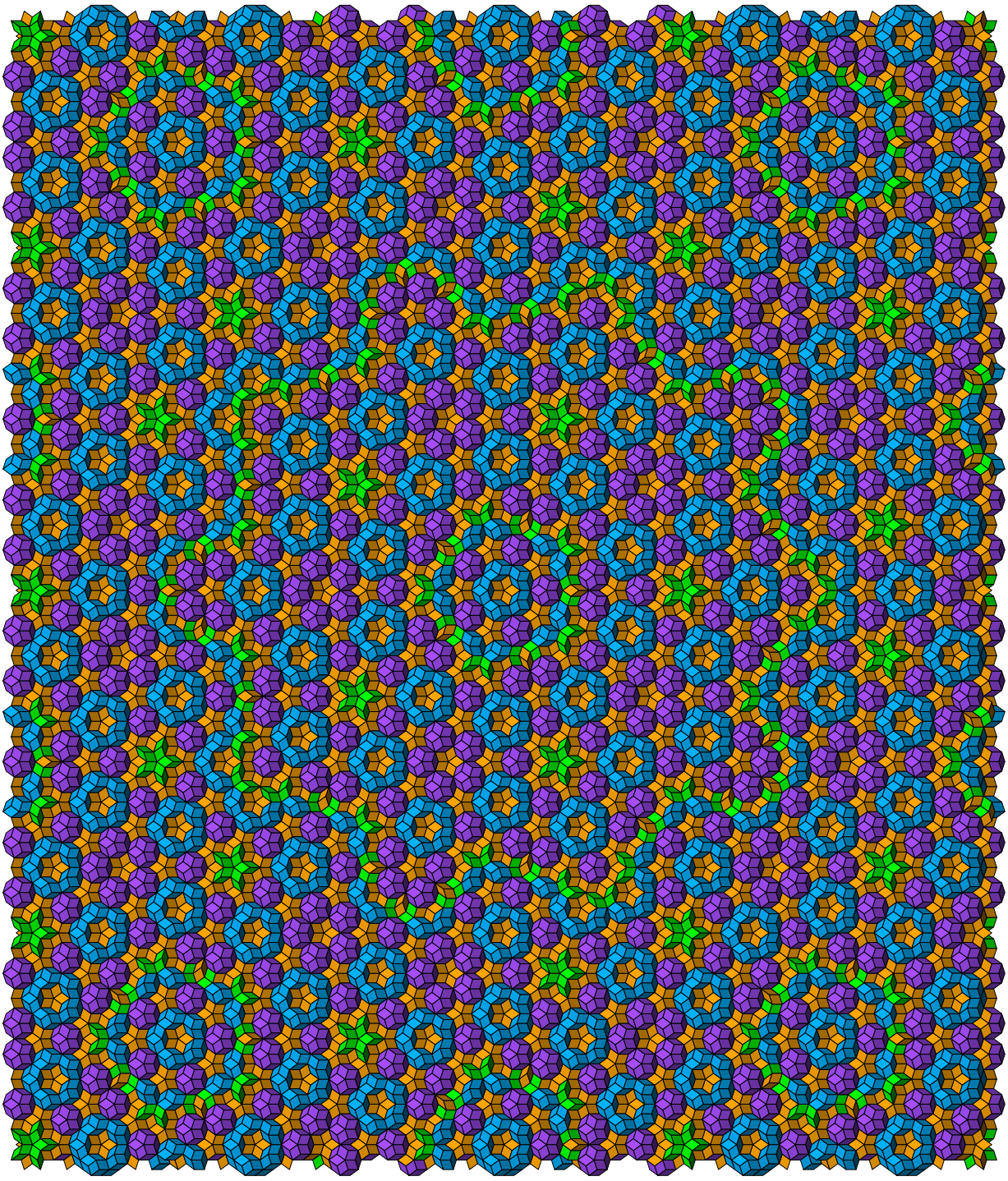

Figure 3. Icosahedral packing of zonohedra. The packing is centered at the type *A* node, and the layer is cut perpendicular to the 5-fold axis. The second layer of polyhedra is shown.

prolate rhombohedron has a unit volume and the volumes of all other zonohedra are related as $1 : 2\tau : 5\tau : 10\tau$.

$$\begin{pmatrix} 21 & 3 & 2\frac{2}{5} & 1\frac{3}{5} \\ 68 & 11 & 6\frac{2}{5} & 5\frac{3}{5} \\ 170 & 20 & 17 & 15 \\ 340 & 30 & 36 & 31 \end{pmatrix} \begin{pmatrix} 1 \\ 2\tau \\ 5\tau \\ 10\tau \end{pmatrix} = \tau^9 \begin{pmatrix} 1 \\ 2\tau \\ 5\tau \\ 10\tau \end{pmatrix}.$$

The scale factor for the Socolar–Steinhardt tiling is τ^3 and corresponds to the aspect ratio of cells before and after the inflation. Therefore, the volumes of cells increase by a factor of τ^9. The multiplication of $\mathbf{M}^{\mathrm{T}}$ by $\mathbf{v}$ in accordance with the common „row by column“ rule indicates the number and type of polyhedra filling the enlarged supercells. Fractional numbers emerge due to the fact that certain

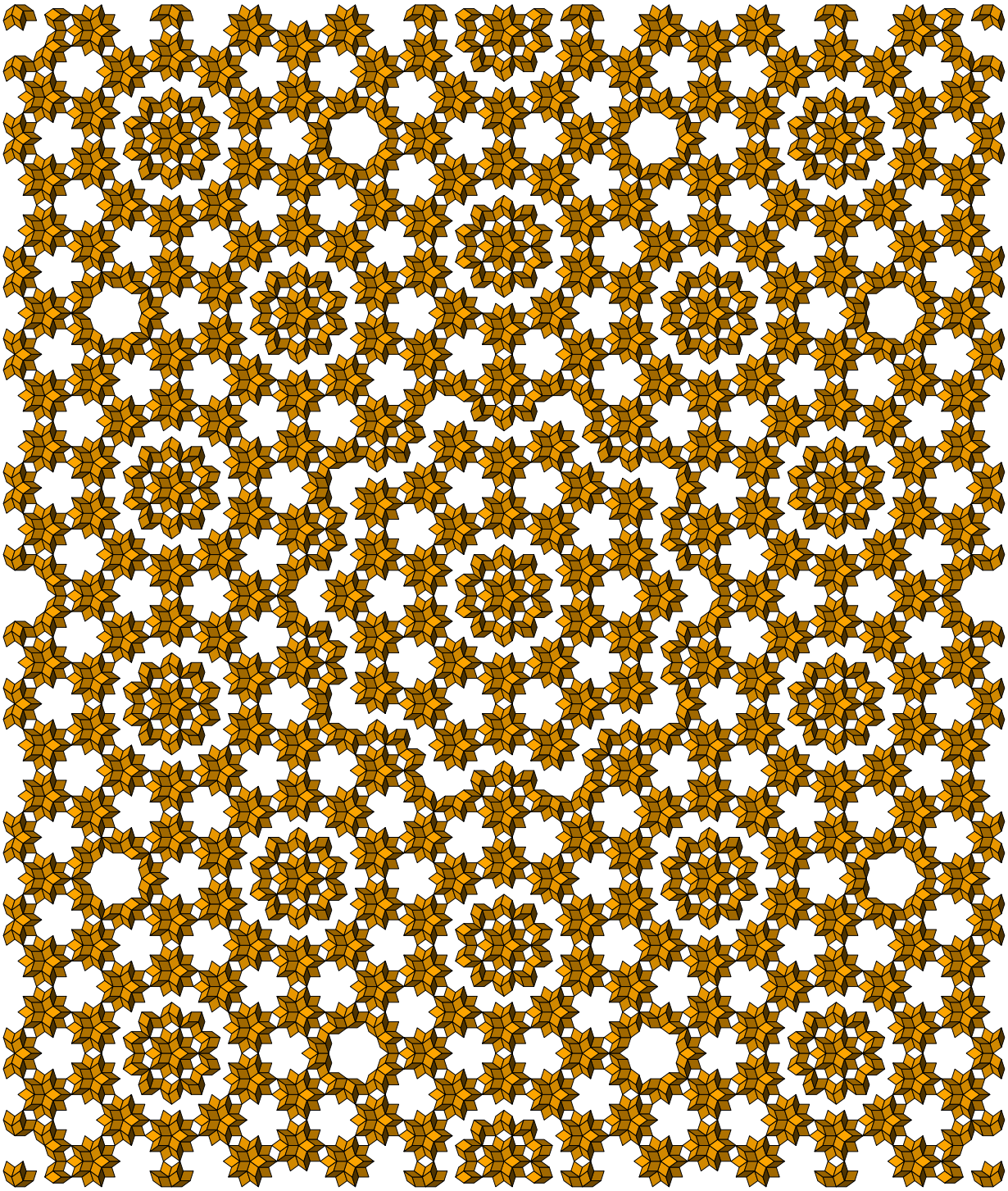

Figure 4. Icosahedral packing of zonohedra. The packing is centered at the type B node, and the layer is cut perpendicular to the 5-fold axis. Only the rhombohedra of the first layer of polyhedra are shown.

cells, being shared by adjacent supercells, are involved in inflation only partially. In our case, it is evident that the multiplication of a matrix by a vector comes down to the multiplication of a vector by a scalar: τ^9 is the Perron–Frobenius eigenvalue and cell volume vector $\mathbf{v}$ is the corresponding right eigenvector.

The next iteration of the inflation–deflation procedure corresponds to repeated left multiplication of this equation by matrix $\mathbf{M}^{\mathrm{T}}$. Raising $\mathbf{M}^{\mathrm{T}}$ to power k, one finds the number of cells of each type after the k-th iteration; the volumes of considered spatial regions increase by a factor of τ^{9k} in this case. This procedure essentially comes

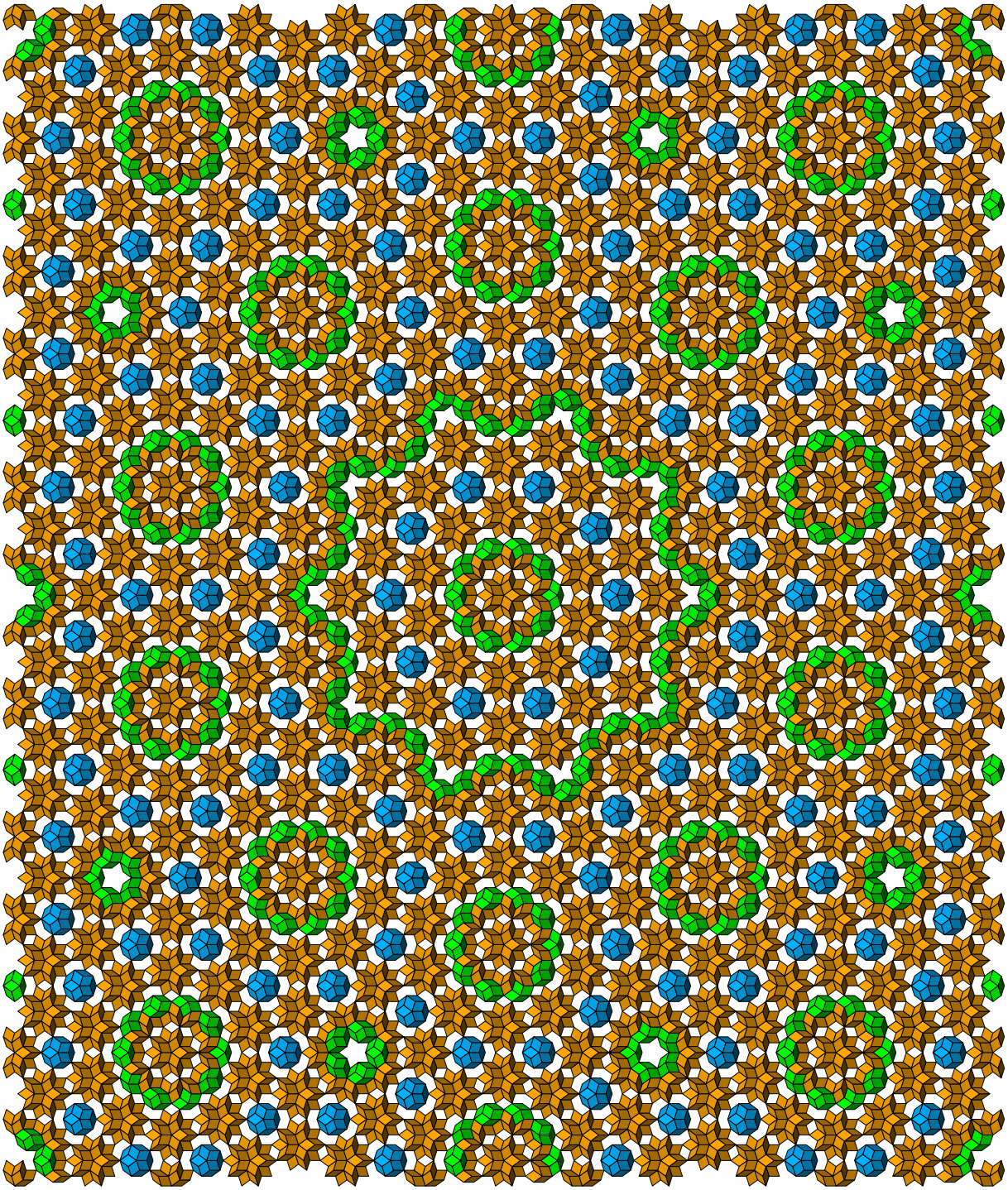

Figure 5. Icosahedral packing of zonohedra. The packing is centered at the type B node, and the layer is cut perpendicular to the 5-fold axis. All polyhedra of the first layer are shown.

down to Perron projection and provides an opportunity to calculate the number of cells of each type in a macroscopic packing normalized to unit volume (the volume of a unit rhombohedron). Application of the Perron projection to matrix $\mathbf{M}^{\mathrm{T}}$ results in the direct product of its right and left eigenvectors $\mathbf{v}$ and $\mathbf{w}$, respectively. Left eigenvector $\mathbf{w}$ is the desired probability vector (indicates the relative number of cells of each type in a global packing):

$$\lim_{k\to\infty}\left(\frac{1}{\tau^9}\,\mathbf{M}^{\mathrm{T}}\right)^k = \mathbf{v}\otimes\mathbf{w},$$

$$\mathbf{v}^{\mathrm{T}} = (1,\ 2\tau,\ 5\tau,\ 10\tau),$$

$$\mathbf{w}^{\mathrm{T}} = \frac{1}{10}\,(6-2\tau,\ -11+7\tau,\ 10-6\tau,\ -3+2\tau).$$

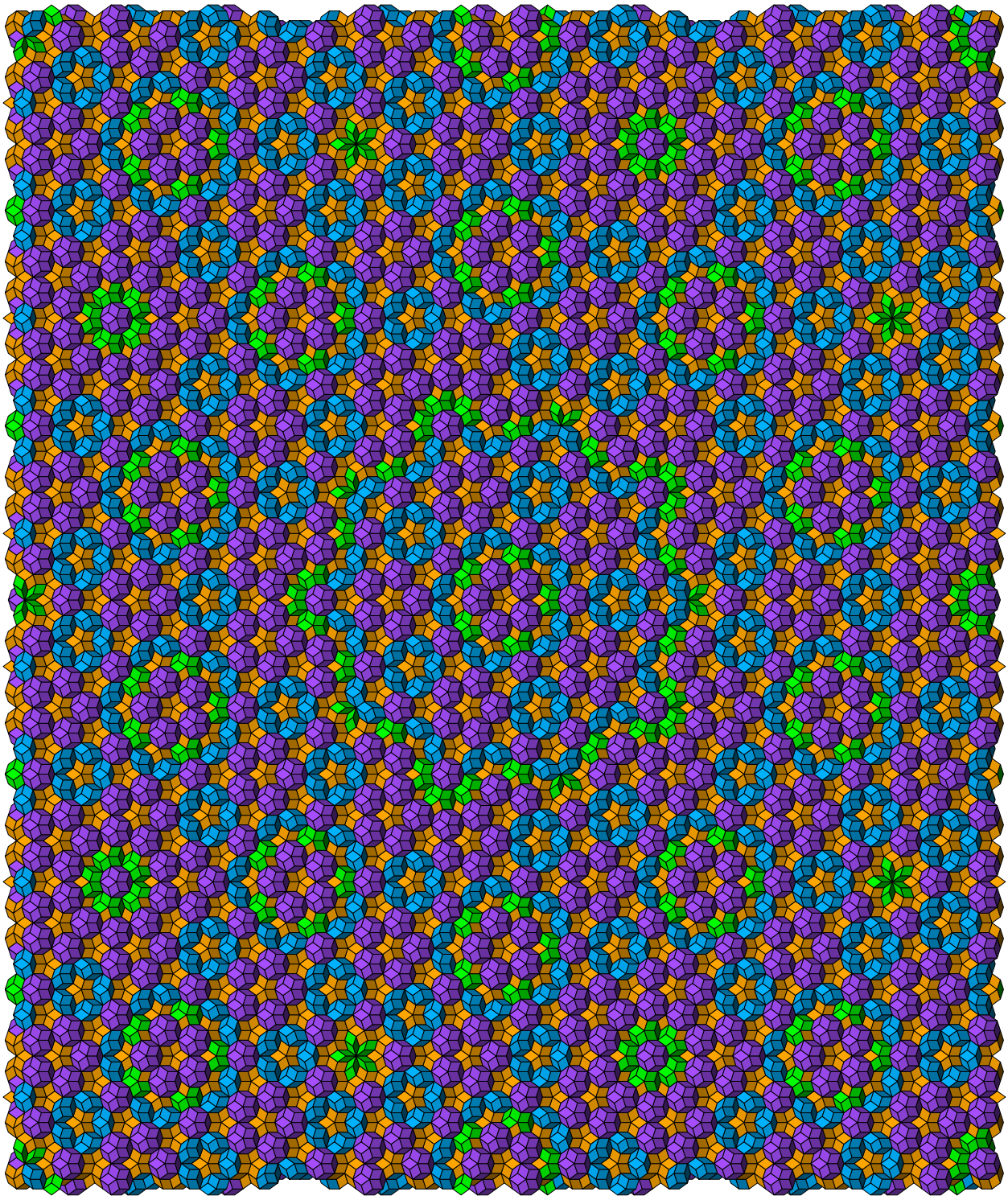

Figure 6. Icosahedral packing of zonohedra. The packing is centered at the type *B* node, and the layer is cut perpendicular to the 5-fold axis. The second layer of polyhedra is shown.

Having completed the Perron projection, we obtain a degenerate matrix. The first row of this matrix provides the probabilities for each type of cells normalized to unit volume of a prolate rhombohedron. The relative number of each type of cells normalized to the volume of a rhombic dodecahedron is found in the second row. The third row provides the number of cells normalized to the volume of a rhombic icosahedron. The last (fourth) row provides the number of cells normalized to the volume of a triacontahedron.

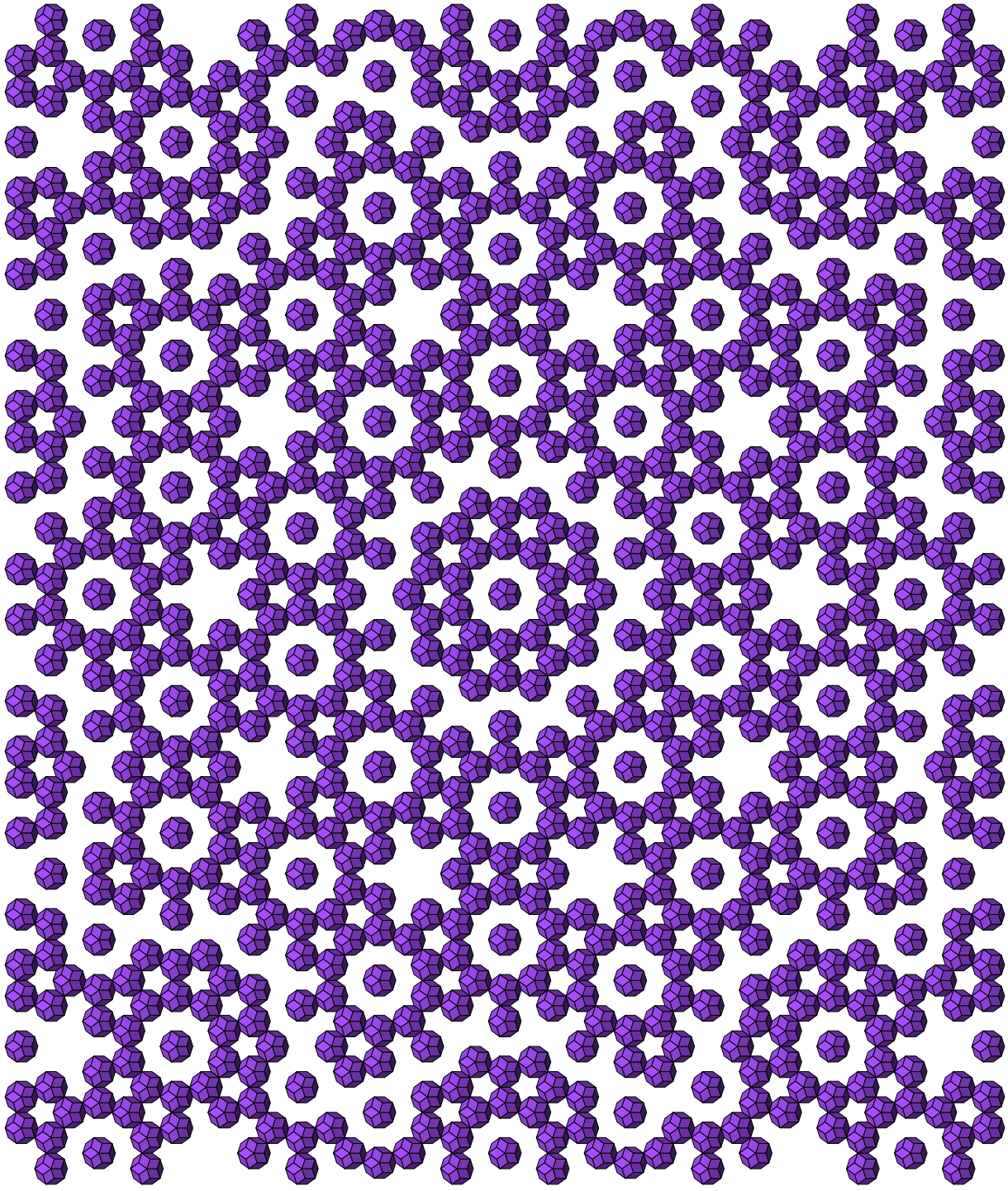

Figure 7. Icosahedral packing of zonohedra. The packing is centered at the type C node, and the layer is cut perpendicular to the 5-fold axis. Only the triacontahedra of the first layer of polyhedra are shown.

The key finding of the present study is that a similar procedure may be used for averaging of virtually any function depending explicitly on volume.

Specifically, the intensity of diffraction peaks is assumed to be directly proportional to the scattering volume within the kinematic theory of diffraction. In the case of a common periodic crystal, the intensity of a reflection with Miller indices $\{hkl\}$ is assumed to be directly proportional to the squared modulus of the structure factor F_{hkl}. This factor is, in turn, calculated by summing the atomic scattering factors with the corresponding phase factors over all atoms in a unit cell. This corresponds to normalization to a unit cell volume. Is it possible to calculate certain „partial“ structure factors for each type of unit cells in a quasicrystal and average the

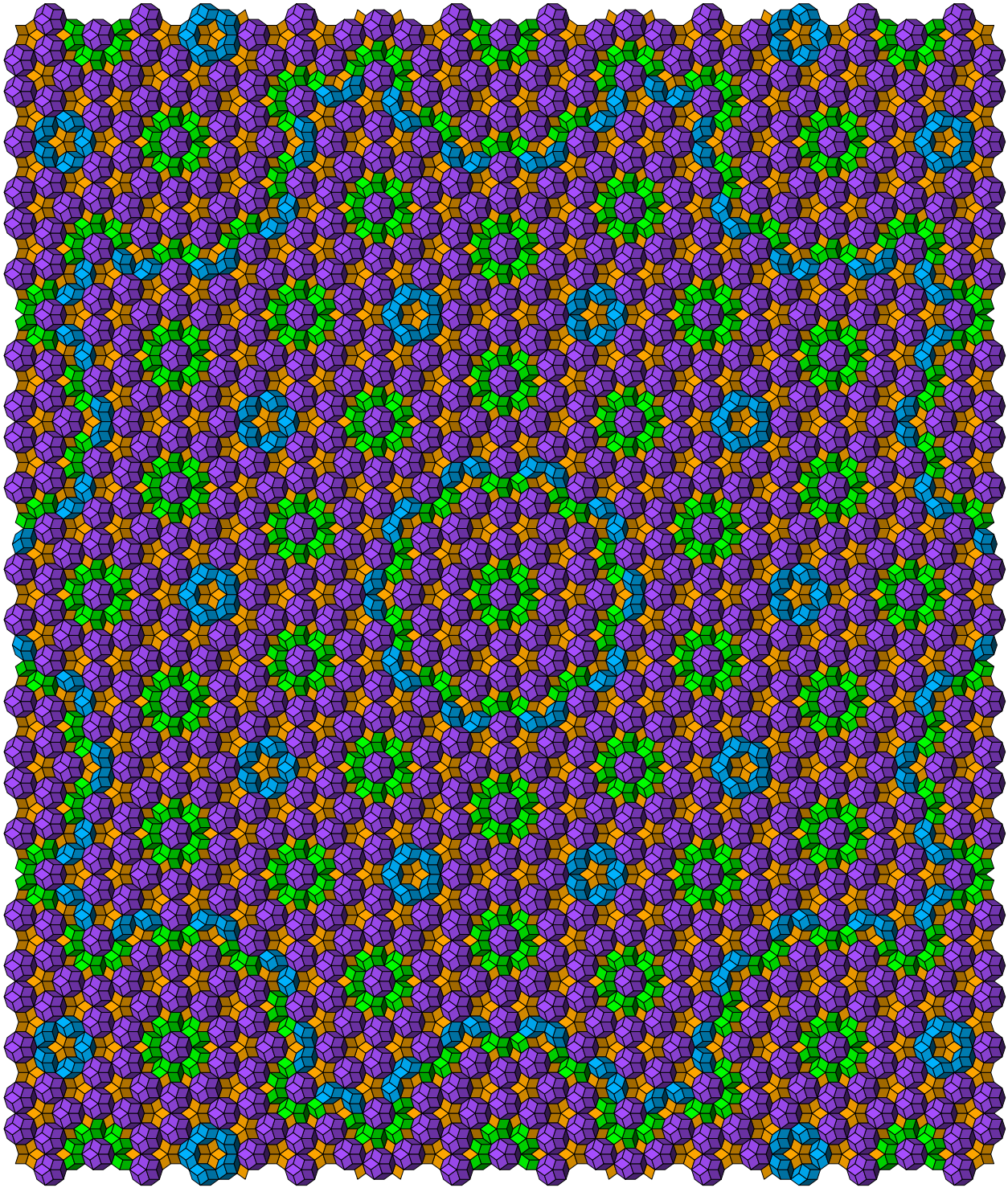

Figure 8. Icosahedral packing of zonohedra. The packing is centered at the type C node, and the layer is cut perpendicular to the 5-fold axis. All polyhedra of the first layer are shown.

obtained values over the entire quasicrystal volume using the inflation–deflation algorithm? In other words, a question arises: is it possible to completely abandon the higher-dimensional approach?

According to our preliminary estimates [20], the calculation of intensities of diffraction reflections within the concept of unit cells is feasible, but the averaging procedure is much more complex in this case. Owing to the emergence of phase factors, one needs to take into account not just four types of cells in standard orientations, but all orbits of all cells (i.e., $20 + 30 + 12 + 1 = 63$ variants of cells with all their possible orientations factored in).

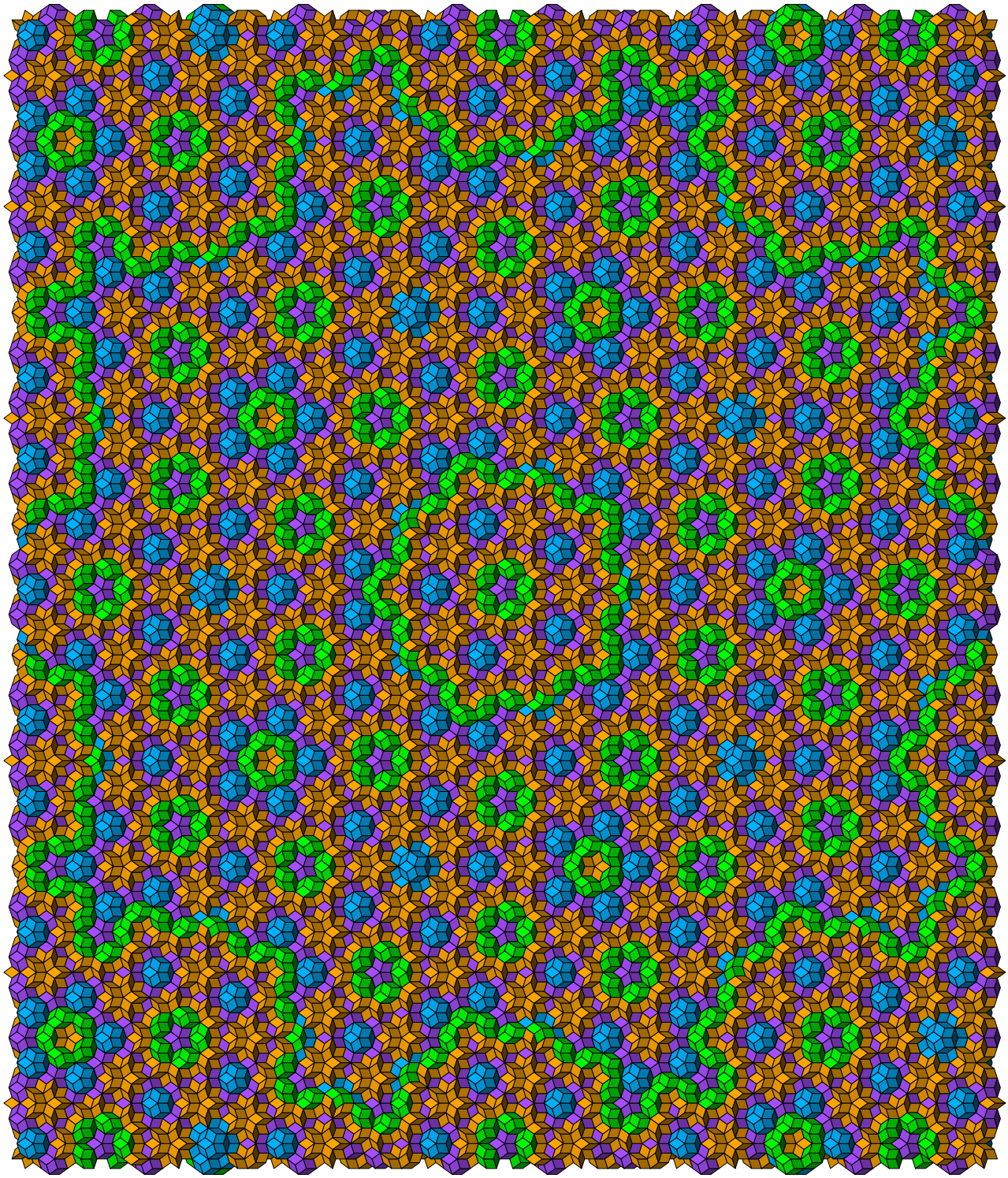

Figure 9. Icosahedral packing of zonohedra. The packing is centered at the type C node, and the layer is cut perpendicular to the 5-fold axis. The second layer of polyhedra is shown.

Let us clarify the principle of this method. We fill unit cells with specific atoms and consider a diffraction reflection for a certain scattering vector **H**. As in the higher-dimensional approach, it is characterized by six integer indices, but is a three-dimensional vector by nature. Let us calculate the partial structure factors of four types of cells with all their possible orientations factored in (this calculation is a perfect analogy with the one for structure factors of a common periodic crystal). We perform inflation and deflation of cells and consider the structure factors of

newly formed enlarged supercells. It is evident that the sum over all atoms in a supercell may be split into sums over subcells. In other words, the partial structure factors of supercells are linear combinations of partial structure factors of constituent subcells, and the corresponding coefficients are specified by substitution rules. Cells consist of atoms, while supercells consist of subcells. The formulae for calculation of structure factors remain unchanged, but the partial structure factors of subcells need to be used instead of atomic form factors.

Thus, calculating the structure factors of supercells, we arrive at a similar problem of averaging over volume, where the volume of considered regions increases by a factor of τ^9 with each iteration. The only difference is that the entries of the corresponding matrix are not real but complex numbers and phase factors vary from one iteration to the next one [20]. The structure factor calculation reduces to calculation of a column vector of partial structure factors of cells and systematic application of the iterative averaging algorithm. At each step of this algorithm, a special 63×63 matrix is calculated in accordance with substitution rules and multiplied by the column vector obtained at the previous iteration. After that, the entries of the column vector are normalized to the initial unit cell volumes. At the end stage of the algorithm, all entries of the column vector of structure factors correspond to one and the same average value. In practice, one can take any of them. The first entries corresponds to normalization to a unit rhombohedron volume, while the last one is 10τ times greater (in magnitude), since it corresponds to normalization to the volume of a triacontahedron, which is larger. Average structure factor $F_{\mathbf{H}}$ obtained this way characterizes an icosahedral quasicrystal as a whole (under the assumption that its structure may be presented as a self-similar packing of several types of unit cells). It is exactly similar in nature to structure factor F_{hkl} of a common periodic crystal in classical crystallography.

We have tested the method for several relatively simple packing variants differing by the scheme of filling the cells with specific atoms. The algorithm was found to converge fairly rapidly in all these cases. This suggests that the calculation of peak intensities by averaging of partial structure factors of cells may become a viable alternative to the method of projection from 6*D*-space.

Conclusion

The concept of (quasi-) unit cells is proposed as an alternative to the higher-dimensional approach in characterization of the structure of icosahedral quasicrystals. The proposed method of characterization with unit cells is equivalent to the one used for periodic crystals. The difference is that four unit cells need to be used instead of a single one and an iterative inflation and deflation algorithm should be used instead of translations to fill the entire space with cells. Icosahedral packings are characterized as lists of cells with the type, position, and orientation specified for each cell. Fairly large patterns of all three types of the Socolar–Steinhardt packing, which illustrate the key structural features and hierarchical motifs of icosahedral quasicrystals, were generated with the use of the developed algorithm. The viability of calculation of the reflex intensities in the structure analysis of quasicrystals without the use of higher-dimensional crystallography techniques was demonstrated. In order to do that, one needs first to calculate partial structure factors for each type of unit cells and then average them over the quasicrystal volume in accordance with the derived substitution rules.

Funding

This study was supported by the Russian Science Foundation (grant No. 23-23-00392, https://rscf.ru/project/23-23-00392/).

Conflict of interest

The authors declare that they have no conflict of interest.

References

[1] D. Shechtman, I. Blech, D. Gratias, J.W. Cahn. Phys. Rev. Lett., **53**, 70 (1984). DOI: 10.1103/PhysRevLett.53.1951
[2] D. Levine, P.J. Steinhardt. Phys. Rev. B, **34**, 596 (1986). DOI: 10.1103/PhysRevB.34.596
[3] J.E.S. Socolar, P.J. Steinhardt. Phys. Rev. B, **34**, 617 (1986). DOI: 10.1103/PhysRevB.34.617
[4] P. Kramer, R. Neri. Acta Cryst. A, **40**, 580 (1984). DOI: 10.1107/S0108767384001203
[5] W. Steurer, S. Deloudi. *Crystallography of Quasicrystals. Concepts, Methods and Structures* (Springer, Berlin-Heidelberg, 2009), DOI: 10.1007/978-3-642-01899-2
[6] A. Yamamoto, H. Takakura, A.-P. Tsai. Phys. Rev. B, **68**, 094201 (2003). DOI: 10.1103/PhysRevB.68.094201
[7] H. Takakura, C. Pay Gómez, A. Yamamoto, M. de Boissieu, A.-P. Tsai. Nature Mater., **6**, 58 (2007). DOI: 10.1038/nmat1799
[8] T. Yamada, H. Takakura, H. Euchner, C. Pay Gómez, A. Bosak, P. Fertey, M. de Boissieu. IUCrJ, **3**, 247 (2016). DOI: 10.1107/S2052252516007041
[9] W. Man, M. Megens, P.J. Steinhardt, P.M. Chaikin. Nature, **436**, 993 (2005). DOI: 10.1038/nature03977
[10] S.V. Boriskina. Nat. Photon., **9**, 422 (2015). DOI: 10.1038/nphoton.2015.107
[11] S.-Y. Jeon, H. Kwon, K. Hur. Nat. Phys., **13**, 363 (2017). DOI: 10.1038/nphys4002
[12] A. Poddubny, E. Ivchenko. Phys. E: Low-Dimens. Syst. Nanostructur., **42**, 1871 (2010). DOI: 10.1016/j.physe.2010.02.020
[13] A.D. Sinelnik, I.I. Shishkin, X. Yu, K.B. Samusev, P.A. Belov, M.F. Limonov, P. Ginzburg, M.V. Rybin. Adv. Opt. Mater., **8**, 2001170 (2020). DOI: 10.1002/adom.202001170
[14] Y. Nagaoka, J. Schneider, H. Zhu, O. Chen. Matter., **6**, 30 (2023). DOI: 10.1016/j.matt.2022.09.027
[15] M. Baake, U. Grimm. Acta Cryst. A, **76**, 559 (2020). DOI: 10.1107/S2053273320007421

[16] A.E. Madison. RSC Adv., **5**, 5745 (2015). DOI: 10.1039/C4RA09524C
[17] A.E. Madison. RSC Adv., **5**, 79279 (2015). DOI: 10.1039/C5RA13874D
[18] A.E. Madison. Struct. Chem., **26**, 923 (2015). DOI: 10.1007/s11224-014-0559-3
[19] A.E. Madison, P.A. Madison. Proc. Roy. Soc. A, **475**, 20180667 (2019). DOI: 10.1098/rspa.2018.0667
[20] A.E. Madison, P.A. Madison. Struct. Chem., **31**, 485 (2020). DOI: 10.1007/s11224-019-01430-w
[21] D.A. Rabson, N.D. Mermin, D.S. Rokhsar, D.C. Wright. Rev. Mod. Phys., **63**, 699 (1991). DOI: 10.1103/RevModPhys.63.699

Translated by D.Kondaurov